Accelerated Publications

Active Site Mutants Implicate Key Residues for Control of Color and Light Cycle Kinetics of Photoactive Yellow Protein†

Ulrich K. Genick,‡ Savitha Devanathan,§ Terry E. Meyer,§ Ilona L. Canestrelli,‡ Erica Williams,‡ Michael A. Cusanovich,§ Gordon Tollin,§ and Elizabeth D. Getzoff*,‡

Department of Molecular Biology, The Scripps Research Institute, 10550 North Torrey Pines Road, La Jolla, California 92037, and Department of Biochemistry, University of Arizona, Tucson, Arizona 85721

Received September 11, 1996; Revised Manuscript Received November 12, 1996⊗

ABSTRACT: To understand how the protein and chromophore components of a light-sensing protein interact to create a light cycle, we performed time-resolved spectroscopy on site-directed mutants of photoactive yellow protein (PYP). Recently determined crystallographic structures of PYP in the ground and colorless I2 states allowed us to design mutants and to study their photosensing properties at the atomic level. We developed a system for rapid mutagenesis and heterologous bacterial expression for PYP apoprotein and generated holoprotein through formation of a covalent thioester linkage with the *p*-hydroxycinnamic acid chromophore as found in the native protein. Glu46, replaced by Gln, is buried in the active site and hydrogen bonds to the chromophore's phenolate oxygen in the ground state. The Glu46Gln mutation shifted the ground state absorption maximum from 446 to 462 nm, indicating that the color of PYP can be fine-tuned by the alteration of hydrogen bonds. Arg52, which separates the active site from solvent in the ground state, was substituted by Ala. The smaller red shift (to 452 nm) of the Arg52Ala mutant suggests that electrostatic interactions with Arg52 are not important for charge stabilization on the chromophore. Both mutations cause interesting changes in light cycle kinetics. The most dramatic effect is a 700-fold increase in the rate of recovery to the ground state of Glu46Gln PYP in response to a change in pH from pH 5 to 10 ($pK_a = 8$). Prompted by this large effect, we conducted a careful re-examination of pH effects on the wild-type PYP light cycle. The rate of color loss decreased about 3-fold with increasing pH from pH 5 to 10. The rate of recovery to the colored ground state showed a bell-shaped pH dependence, controlled by two pK_a values (6.4 and 9.4). The maximum recovery rate at pH 7.9 is about 16 times faster than at pH 5. The effect of pH on Arg52Ala is like that on wild type except for faster loss of color and slower recovery. These kinetic effects of the mutations and the changes with pH demonstrate that both phases in PYP's light cycle are actively controlled by the protein component.

To facilitate sensitivity of light detection and efficient elicitation of a biological response, a photoreceptor protein has to fine-tune both the absorption spectrum of its chromophore and the kinetics of its light cycle. Photoactive yellow protein (PYP),[1] for which high-resolution structural information is available, is an ideal system for studying these forces in atomic detail. PYP was originally isolated from *Ectothiorhodospira halophila* (Meyer, 1985). The similarity between the visible absorption spectrum of PYP and the wavelength dependence of the negative phototactic response implicates PYP as the receptor responsible for this effect (Sprenger et al., 1993). Recently, PYP homologs were also discovered in two other species of halophilic phototrophic bacteria (Koh et al., 1996), suggesting that PYPs may be widespread in this class of bacteria. Unlike the well-known light receptors rhodopsin (Schertler et al., 1993), bacteriorhodopsin (Henderson et al., 1990), and sensory rhodopsin (Bogomolni & Spudich, 1982; Oesterhelt et al., 1992), which are all integral membrane proteins, PYP is a small (14 kDa), water soluble, cytoplasmic protein. The *p*-hydroxycinnamyl chromophore is bound via a thioester bond (Baca et al., 1994; Hoff et al., 1994a) to Cys69, the sole cysteine in PYP (Van Beeumen et al., 1993). The 1.4 Å X-ray structure of PYP in the ground state (Borgstahl et al., 1995) shows the *trans* isomer of the chromophore buried in the hydrophobic core. On one side, the chromophore is separated from the solvent only by Arg52, which is tethered by hydrogen bonds. The chromophore's phenolic oxygen is hydrogen bonded to Tyr42 and Glu46. The active site has been shown to stabilize the chromophore as the deprotonated phenolate anion (Baca et al., 1994; Kim et al., 1995), indicating that the ionization constants for both Glu46 and the chromophore are shifted substantially from their solution pK_a values (4.5 and 9). Upon acid titration, PYP retains the yellow color characteristic of

† This work was supported in part by grants from the NIH (GM37684 and GM21277) and USAF Rome Laboratory (F3060295C0100) and a scholarship from the Boehringer Ingelheim Fonds for U.K.G.

* To whom correspondence should be addressed.

‡ The Scripps Research Institute.

§ University of Arizona.

⊗ Abstract published in *Advance ACS Abstracts,* December 15, 1996.

[1] Abbreviations: PYP, photoactive yellow protein; PCR, polymerase chain reaction; OD, optical density; IPTG, isopropyl β-D-thiogalactopyranoside; Tris, tris(hydroxymethyl)aminomethane; EDTA, ethylenediaminetetraacetic acid; SDS−PAGE, sodium dodecyl sulfate−polyacrylamide gel electrophoresis; HEPES, *N*-(2-hydroxyethyl)-piperazine-*N*′-2-ethanesulfonic acid; MES, 2-(*N*-morpholino)ethanesulfonic acid.

S0006-2960(96)02288-X CCC: $14.00

the negatively charged protein-bound chromophore until reaching a solution pH of 2.7. Below this pH, PYP is completely colorless even in the absence of actinic light (Meyer, 1985). When ground state PYP (P; $\lambda_{max} = 446$ nm) captures a photon, the electronically excited state (P*) is rapidly (<10 ns) converted into the red-shifted intermediate (I1; $\lambda_{max} = 460-465$ nm), which then proceeds to a second intermediate (I2; $\lambda_{max} = 340-355$ nm) on a millisecond time scale (Meyer et al., 1987; Hoff et al., 1994b). Formation of the colorless intermediate (I2) is accompanied by the uptake of a proton from the solvent (Meyer et al., 1993). Intermediate I2 returns back to the ground state in a relatively slow reaction (seconds), releasing a proton to complete its self-contained photocycle.

MATERIALS AND METHODS

Cloning of the pyp Gene. The *pyp* gene was cloned from a vector of a library containing *Pst*I fragments of genomic DNA from *E. halophila* (Baca et al., 1994). The vector was used as a template for a PCR reaction with the primers 5′CCCCCCATGGAACACGTAGCCTTCGGTAGC3′ and 5′CCCGGATCCCTACTAGACGCGCTTGACGAA3′ to attach *Nco*I and *Bam*HI restriction sites for integration of the gene into a pet20b expression vector (Novagen Inc.). An Applied Biosystems automated sequencer was used to confirm the expected sequence of the construct. Sequencing conditions were adapted as described before (Baca et al., 1994) to compensate for high GC content of the *pyp* gene. As expected, the *pyp* gene was inserted between the *Nco*I and *Bam*HI site, placing it behind the *pelB* leader sequence furnished by the vector. The resulting vector, containing the wild-type *pyp* gene, will be referred to as pPYP.

Site-Directed Mutagenesis. Mutagenesis of the *pyp* gene was performed by PCR following the protocol of Landt et al. (1990). The pPYP template was used with the same terminal primers as those used for the PCR-mediated integration into the expression vector. The mutagenic primers were 5′GCGACATCACCGGC*GCT*GACCCGAAGCAGT3′ for the Arg52Ala mutation and 5′AGTACAACGCCGCG*CAG*GGCGACATCACCG3′ for the Glu46Gln mutation. The final PCR products were cloned into the pet20b vector. The two mutant *pyp* genes were then sequenced as described for the wild-type gene, and the expected sequences were confirmed.

Protein Expression. The pPYP vector was transferred into *Escherichia coli* cells of strain BL21 (DE3) (Novagen Inc.). The transformed cells were grown in a laboratory shaker at 37 °C in a medium containing 10 g/L Bacto Tryptone (Difco), 6.27 g/L dibasic potassium phosphate, 6 g/L dibasic sodium phosphate heptahydrate, 5 g/L sodium chloride, 4.15 g/L monobasic potassium phosphate, 4 g/L glucose, 1.32 g/L magnesium sulfate, and 1 g/L ammonium chloride until they reached an OD at 600 nm of ∼0.6. Then, protein expression was induced by addition of IPTG to the media to a final concentration of 0.1 mM. After 2 h, the cells were separated from the apo-PYP-containing growth medium by centrifugation.

Chromophore Attachment and Protein Purification. Fresh carbonyl diimidazole (120 mg) (Aldrich) was used to activate 105 mg of *p*-hydroxycinnamic acid (Sigma) in 18 mL of tetrahydrofuran (tetrahydrofuran was purified on a column of Brockman grade 1 aluminum oxide) by stirring for ∼1 h at room temperature. Tetrahydrofuran was removed by evaporation and the product dissolved in water. Activated chromophore was added to 3 L of growth medium immediately after the removal of cells. The reaction mixture was kept at room temperature for 2−3 h. The purification of PYP was carried out at 4 °C. The growth medium was concentrated to a volume of approximately 200 mL by lateral flow filtration (Millipore) using a 5000 MW cutoff membrane. The concentrate was dialyzed overnight against 4 L of buffer [50 mM Tris (pH 7.5) and 2 mM EDTA (Tris-EDTA)] at 65% saturated ammonium sulfate. The precipitate was removed by centrifugation, and the supernatant was dialyzed against the same buffer containing no ammonium sulfate. The sample was concentrated to a volume of ∼30 mL by membrane filtration using a YM10 membrane (Amicon). The concentrate was purified over a Superdex 75 (Pharmacia) sizing column eluted with Tris-EDTA buffer containing 150 mM sodium chloride. Yellow fractions were pooled, dialyzed against Tris-EDTA buffer, concentrated, and loaded onto a Poros-HQ anion exchange column (PerSeptive Biosystems). The column was eluted with Tris-EDTA buffer containing a concentration gradient of 0 to 1.0 M NaCl. Purity was checked by SDS−PAGE and isoelectric focusing. The protein was dialyzed against 20 mM HEPES buffer (pH 7.0) and concentrated to ∼20 mg/mL. Flash-frozen samples of purified PYP were stored at −80 °C.

N-Terminal Sequencing. The first six residues of recombinantly expressed PYP apoprotein were sequenced by Edman degradation on a Perkin-Elmer/Applied Biosystems Division model 492A protein sequencer using 5 pmol of purified protein as a sample.

Optical Spectroscopy. UV−visible spectroscopy under a broad range of buffer conditions was performed on a Hewlett-Packard model 8453 diode array spectrophotometer at room temperature.

Time-Resolved Optical Spectroscopy. The laser flash photolysis and spectroscopy apparatus and the methods used for data analysis were as previously described (Meyer et al., 1987). The PYP samples were transferred into different buffers ranging in pH from 5 to 10. Buffers were 20 mM MES (pH 5−6.5), 20 mM HEPES (pH 6.5−8.5), and 20 mM glycine (pH 8.5−10). All samples used for time-resolved spectroscopy were adjusted for identical absorption at 446 nm and checked for changes in the ground state absorption spectra due to different buffer conditions. Proton uptake in samples of PYP during the light cycle was determined by time-resolved spectroscopic monitoring of color changes in bromo-cresol purple, a pH-sensing dye with a pK_a of 6.3, as previously described for native PYP (Meyer et al., 1993).

Protein Stability, Secondary Structure, and Circular Dichroism. Protein stability was assessed by denaturation of 1 μM solutions of PYP in 20 mM Tris-chloride buffer (pH 7.5) plus 40 mM sodium chloride, with increasing concentrations of guanidine (USB, ultrapure) following a procedure developed by Pace (1975; Meyer et al., 1987). Unfolding was monitored by loss of visible color recorded with a Hewlett Packard Model 8452 diode array spectrophotometer and by changes in the molar ellipticity at 222 nm measured by an AVIV Instruments-modified Cary 60 spectropolarimeter. Secondary structure was measured by far-UV circular dichroism in water using 1 μM protein solutions. Visible circular dichroism was measured in 20

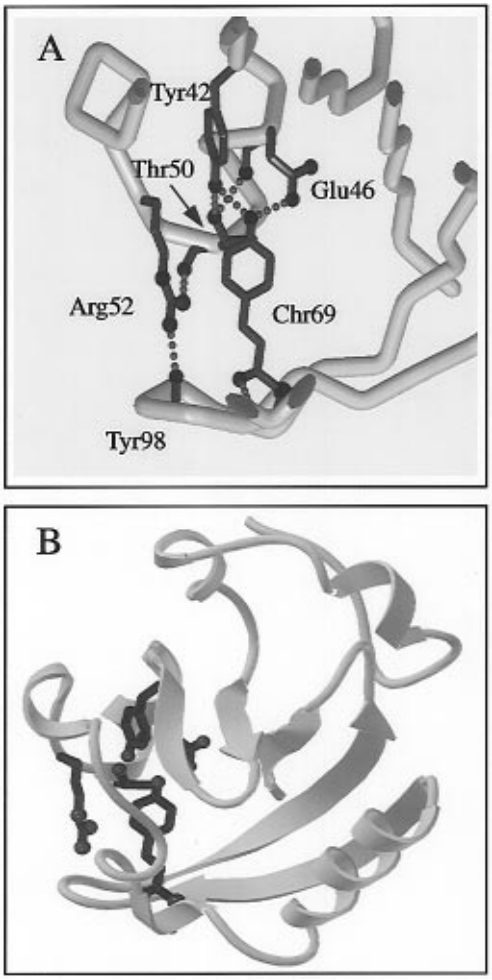

FIGURE 1: (A) Three-dimensional arrangement of active site residues in the ground state. (B) Location of the active site in the overall structure of PYP. Active site residues discussed in this report and main chain atoms that are involved in hydrogen bonds to those residues are shown as dark gray ball and stick figures. Heteroatoms are symbolized by spheres. A chain trace of the protein backbone is shown in light gray. Hydrogen bonds are shown as dotted lines.

mM HEPES adjusted to pH 7 and 9. The protein concentration was 20 μM.

RESULTS

Design of Site-Directed Mutants. Site-directed mutants at Glu46 and Arg52 were designed on the basis of analysis of the three-dimensional structures of PYP in the ground (P) (Borgstahl et al., 1995) and colorless (I2) (Genick et al., 1997) states. Figure 1 shows the active site and its location in the overall structure of PYP. Glu46 was selected for its unusual location and hydrogen-bonding properties. It is completely buried in the hydrophobic core and hydrogen bonds to the chromophore's phenolate oxygen with one of its carboxyl oxygen atoms, while the other carboxyl oxygen atom has no hydrogen-bonding partner. Unsatisfied hydrogen-bonding valences are quite unusual. Functional groups in folded proteins normally satisfy their hydrogen-bonding valences by bonding to either other protein components, cofactors, or solvent. The unusual hydrogen bonding of Glu46 might be partly responsible for the dramatic shifts in pK_a, relative to their solution values, that both Glu46 and the chromophore's phenolic oxygen experience in the active site. Protonation of the Glu46 side chain is required to avoid electrostatic repulsion from the chromophore's negatively charged phenolate oxygen. Thus, the active site chemical environment must lower the solution pK_a of the chromophore (p$K_a \sim 9$) and/or raise the solution pK_a of the glutamic acid (p$K_a \sim 4.5$) by a total of at least 4.5 pH units. This corresponds to an expenditure of ΔG which equals RT (ΔpK_a) of 2.7 kcal/mol during protein folding to achieve the protonation of Glu46 and the deprotonation of the chromophore observed in the ground state of PYP. This large expenditure of energy suggests that this arrangement of protonation states is likely to be functionally important. Glutamine is the ideal residue to replace Glu46 to test the role of the ionizability of Glu46 for the function of PYP. Glutamine is isosteric to glutamic acid, which reduces the possibility of secondary effects of the mutation resulting from steric clashes or the creation of cavities. The amide group of the Glu46Gln mutant is expected to orient itself such that its nitrogen atom is located closest to the chromophore's phenolic oxygen. This would preserve the existing hydrogen-bonding network. In essence, the Glu46Gln mutation only results in the substitution of an ionizable group by a nonionizable one. Time-resolved crystallographic experiments (Genick et al., 1997) show that Arg52, together with the chromophore, undergoes the largest movement during the formation of the colorless intermediate (I2) and suggest that it is important for the transmission of the light-induced signal to downstream recipients (Borgstahl et al., 1995). Furthermore, the location of Arg52 suggests that it might help stabilize the negative charge on the chromophore by providing electrostatic complementarity. To test this function of Arg52 and to probe the restraints that the large movement of the Arg52 side chain places on the speed of the I1 $\rightarrow$ I2 transition, we chose to truncate this side chain by replacing residue 52 with alanine.

Preparation and Purification of Recombinant PYP Holoprotein. Our new expression system efficiently produces PYP apoprotein and secretes it into the growth medium. As judged by Coomassie blue-stained SDS−PAGE, PYP apoprotein comprises ~80% of the protein in the growth medium after expression but less than 10% of the intracellular protein (data not shown). The best yields of PYP holoprotein were obtained when activated chromophore was added to the apoprotein-containing growth medium immediately after removal of the cells. Growth medium that was stored overnight at 4 °C proved to be much less reactive. Successful attachment of the chromophore could be judged initially by visual inspection of the increased yellow color of the medium. After concentration and purification (see Materials and Methods), this procedure resulted in up to 20 mg of PYP holoprotein per liter of growth medium. Purified protein was better than 95% pure as judged by SDS−PAGE and isoelectric focusing. The high ratio of absorbance at 446 and 280 nm (up to 2.2) (Figure 2) is equal to the best ratios obtained for highly purified PYP from *E. halophila*, indicating that any remaining apo-PYP that had not reacted with chromophore was successfully removed during purification. N-Terminal protein sequencing indicated that cleavage of the signal peptide was complete and the first six residues (MEHVAF) match the wild-type PYP sequence. The procedure for the generation of purified PYP holoprotein described here offers an attractive alternative to other reported methods for chromophore attachment (Imamoto et al., 1995) and *pyp* gene expression (Kort et al., 1996). In particular,

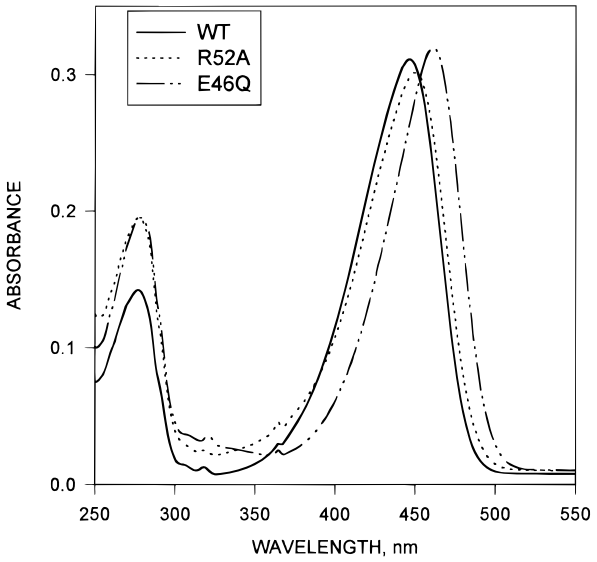

FIGURE 2: Absorption spectra of mutants and recombinant wild-type PYP in 20 mM HEPES buffer at pH 7.

it eliminates the need for the removal of a polyhistidine tag by protease digestion (Kort et al., 1996) which can introduce heterogeneity and proteolytic damage that would be detrimental to crystallization experiments. Secretion of the protein also allows chromophore attachment during protein expression (S. Devanathan et al., unpublished results).

Ground State UV−Visible Spectroscopy of Recombinant Wild-Type and Mutant PYP. Wild-type PYP produced by recombinant expression, followed by chemical attachment of the chromophore, has an absorption spectrum identical to that purified from the natural host (Figure 2). The absorption maximum of the Arg52Ala mutant in the visible region (452 nm) is only slightly red-shifted relative to the absorption maximum of the wild-type protein (446 nm). The visible absorption spectrum of the Glu46Gln mutant is more significantly red-shifted, resulting in an absorption maximum at 462 nm. These same shifts were also observed in the flash-induced time-resolved difference spectra for each of the three proteins (Figure 3). The ground state spectra of wild-type PYP and both of the mutant PYPs were unaffected by changes in the pH over the tested range (pH 5−10).

pH Dependence of Photocycle Kinetics in Native PYP. Previous studies that explored the photocycle kinetics of wild-type PYP at a few pH values detected limited pH dependence (3.5-fold or less) (Meyer et al., 1987). After observing the dramatic pH effects exhibited by the Glu46Gln mutant (described below), we carried out a careful, systematic study of the native protein that covered the entire pH range in which proteins are commonly stable (pH 5−10). Wild-type PYP shows small yet significant pH effects on both the I1 → I2 and the I2 → P transition (Figure 4) as observed previously (Meyer et al., 1987). The rate constant for the I1 → I2 transition decreases about 3-fold over the measured range with a pK_a of ≤5.7. The I2 → P transition displays a much larger, approximately 16-fold, change in its rate constant over the pH 5−10 range, apparently governed by two pK_a values of 6.4 and 9.4. The maximum rate constant for the recovery reaction occurs at pH 7.9. The detailed pH profiles presented here extend and support the previous conclusions of Meyer et al. (1987). In that study, the rate constant for the I1 → I2 transition decreased from pH 5 to 7, while the rate constant for the recovery reaction was

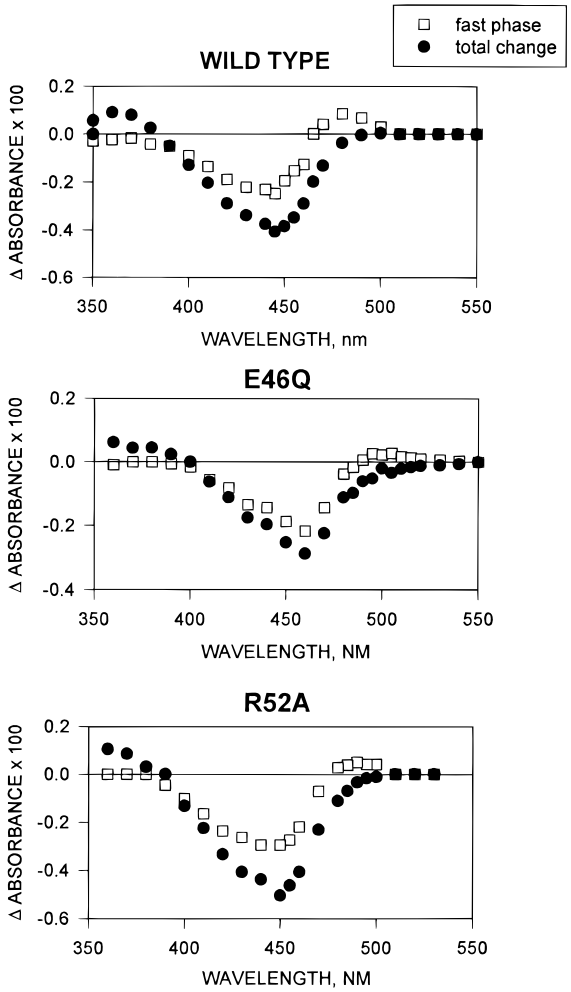

FIGURE 3: Time-resolved flash-induced difference spectra for PYP. The excitation wavelength was 445 nm. The solution contained 20 mM HEPES at pH 7 and 10 μM PYP. The fast phase (□) was obtained by extrapolation of the signal back to the beginning of the second kinetic phase. The total change of the signal (●) corresponds to the absorbance reached prior to decay back to the initial preflash state.

highest near neutral pH. Recombinantly expressed wild-type PYP displays photocycle kinetics that are very similar to those for PYP obtained from the natural host over the pH range from 5 to 10.

Mutational Effects on Photocycle Kinetics. The substitution of Arg52 by alanine affects the rates of both the loss and recovery of color during the photocycle. However, the quantum yield, as judged by the magnitude of the laser-induced photomultiplier signal for samples of identical optical density, containing either wild-type or Arg52Ala PYP, is essentially unaffected. The rate constant for the I1 → I2 conversion at pH 7 is accelerated approximately 3−4-fold from the value for the native or recombinant wild type (3.1−3.9 ms^{-1}) to 12.5 ms^{-1} for the Arg52Ala mutant (Figure 5). In contrast, the speed of the recovery (I2 → P) is decreased 6−8-fold by the same mutation; the rate constant for the I2 → P transition (4.9−6.7 s^{-1}) for native or recombinant wild-type protein decreased to 0.82 s^{-1} for the Arg52Ala mutant (Figure 5). The relative changes in the rate constant due to changes in the pH are quite similar for recombinant wild-type protein and Arg52Ala (Figure 4). This suggests that Arg52 is not responsible for any protonation or deprotonation events that control the speed of the photocycle. The Glu46Gln mutant displayed more radical changes in its

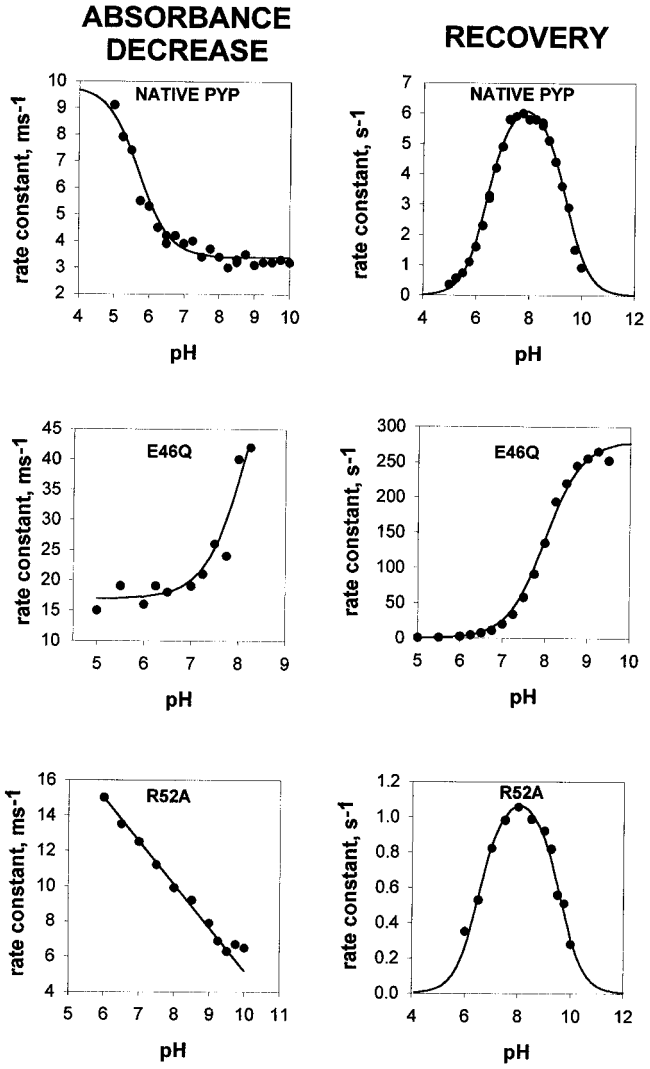

FIGURE 4: Effect of pH on the kinetics of the I1 → I2 transition and recovery of PYP. Note the large differences in scale on the time axis. The buffers were 20 mM MES (pH 5−6.5), HEPES (pH 6.5−8.5), and glycine (pH 8.5−10). Theoretical curves (solid lines) were generated using the equation pH = pK + log A/B and the following parameters: native I1 → I2, 3.4 and 9.8 ms^{-1} (pK = 5.7); native recovery, 0 and 6.3 s^{-1} (pK = 6.4 and 9.4); Glu46Gln I1 → I2, 17 and 67 ms^{-1} (pK = 8.2); Glu46Gln recovery, 0.4 and 280 s^{-1} (pK = 8.0); and Arg52Ala recovery, 0 and 1.1 s^{-1} (pK = 6.5 and 9.6). The data for the I1 → I2 reaction of Arg52Ala could not be fit with the above equation but were connected by a straight line (15 ms^{-1} at pH 6.0 and 5 ms^{-1} at pH 10).

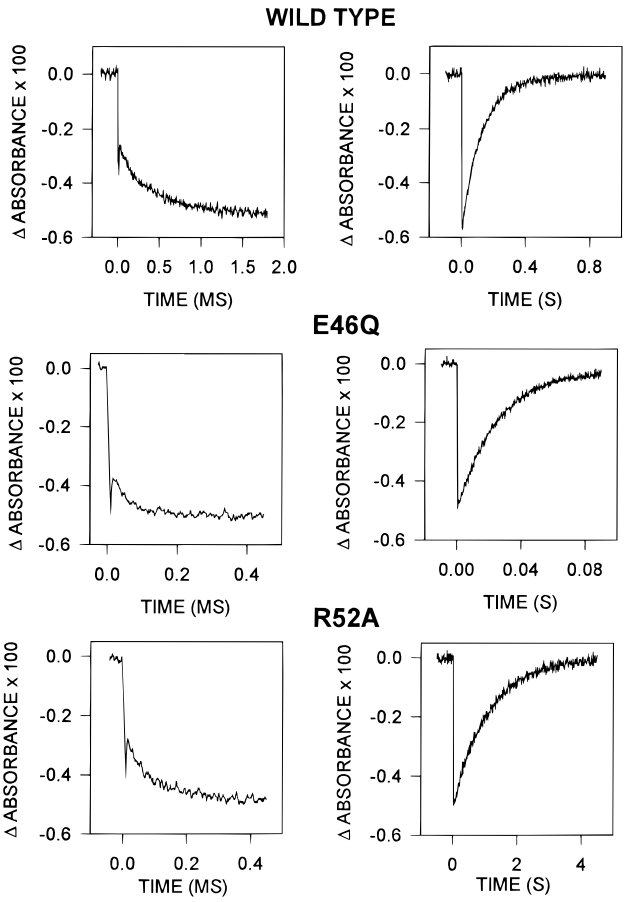

FIGURE 5: Kinetics of light-induced absorbance changes: I1 → I2 reaction (left panels) and recovery (right panels). The conditions match those in Figure 3.

photocycle kinetics than the Arg52Ala mutant, whereas the quantum yield again seemed to be relatively unaffected. At neutral pH, the I1 → I2 conversion in Glu46Gln PYP (rate constant of ∼19 ms^{-1}) is about 5−6 times and the recovery of yellow color (I2 → P) (rate constant of 20 s^{-1}) about 3−4 times faster than for native or recombinant wild-type protein (Figure 5). The most interesting effects of the Glu46Gln mutation lie in the dramatically changed pH dependence of its photocycle reaction rates. Whereas the rate constants for the I2 → P reaction of wild-type and Arg52Ala PYP change ≤16-fold over the pH range from 5 to 10, the same reaction accelerates about 700-fold for the Glu46Gln mutant in the same pH range (Figure 4). The shape of the curve describing the pH dependence of the rate constants has also changed from a bell-shaped curve to a sigmoidal curve, suggesting a pK_a of a single responsible group of approximately 8.0. It is nevertheless possible that the observed shape of the pH dependence curve is simply due to a large shift of the bell-shaped curve observed for wild-type PYP and that the downward part of the curve could not be observed in this study. Increasing the pH beyond 10 degraded the quality of time-resolved optical data (T. E. Meyer and G. Tollin, unpublished results), which we attribute to possible protein denaturation. The rate of the I1 → I2 transition for Glu46Gln PYP, which is also very sensitive to pH changes, accelerates with increasing pH, whereas for wild-type and Arg52Ala PYP, the rate of this transition slows with increasing pH. At pH 8.5, the rate constant for I1 → I2 transition of Glu46Gln exceeds the time resolution of our instrumentation (>50 ms^{-1}). The similarity in the shape of the curves for the pH dependencies of the I1 → I2 transition and the I2 → P transition and the near identity of the pH value at which they occur lead us to suggest that the ionizable group, which is responsible for the pH sensitivity, might be the same for both stages of the photocycle.

Proton Uptake during the Photocycle. Formation of the colorless photocycle intermediate (I2) in light-activated samples of wild-type (Meyer et al., 1993) and both mutant forms of PYP was accompanied by uptake of protons from the solvent, as judged by color changes of the pH sensitive dye bromo-cresol purple (data not shown). Since the pH of the sample had to be adjusted to the pK_a (6.3) of the dye in order to make the measurement, we could not determine the pH dependence of this reaction.

Stability and Secondary Structure. To ensure that changes in the light cycle kinetics caused by the mutations and changes in the pH are not due to indirect effects on global

properties of the protein, we analyzed the overall shape, secondary structure content, and stability of wild-type and mutant PYP proteins. Crystals of recombinant wild-type, Glu46Gln, and Arg52Ala PYP can all be grown under similar conditions from seeds of wild-type protein. These crystals all have similar shapes and dimensions and identical macroscopic symmetry. This suggests a highly similar overall structure of the three proteins. Preliminary X-ray diffraction data for the Glu46Gln mutant reveal a space group and unit cell that are identical to those of wild-type PYP (data not shown).

Monitoring changes in the UV and visible circular dichroism as a function of the concentration of denaturant (guanidinium hydrochloride) yielded energies of unfolding (ΔG_{unfold}) of 7.1 kcal/mol for recombinant wild-type and Glu46Gln PYP. The ΔG_{unfold} of the Arg52Ala mutant is significantly lower (6.2 kcal/mol). We have found previously that destabilization of wild-type PYP by both primary alcohols and urea alters the photocycle kinetics of PYP in a manner similar to that for the Arg52Ala mutant. In both cases, loss of visible color becomes faster and recovery slower (Meyer et al., 1987, 1989). It is possible that the kinetic differences in Arg52Ala PYP may be partially due to the reduced stability of this mutant. A change in the pH from 7 to 9 leaves the secondary structure content of both wild-type and Glu46Gln PYP unchanged as judged by far-UV circular dichroism spectra, indicating that the dramatic pH effects on the photocycle kinetics of Glu46Gln are not caused by large structural rearrangements. The visible circular dichroism spectra of recombinant wild-type and the two mutant proteins are virtually identical to that of native PYP (Meyer et al., 1987), except for the wavelength shifts also observed in the absorption spectra (data not shown). These data suggest minimal or no structural changes in the immediate chromophore environment as a result of the mutations.

DISCUSSION

Protein Control of Ground State Absorption Spectrum. The absorption spectrum of PYP's chromophore bound in the native protein (446 nm) is strongly red-shifted from that of the free protonated chromophore (300 nm) (Baca et al., 1994). Stabilization of a negative charge on the chromophore is one of several mechanisms by which PYP's protein component achieves this red shift (Baca et al., 1994). The remarkable stability of the negative charge indicated by retention of PYP's yellow color to a solution pH of 2.7 (Meyer, 1985) was attributed to the donation of hydrogen bonds from Glu46 and Tyr42 to the chromophore's phenolic oxygen, and counterion stabilization by the positive charge of the guanidinium group of Arg52. Here, we tested this role for Arg52. Removal of the Arg52 guanidinium group in the Arg52Ala mutant slightly red-shifted the visible absorption maximum. In contrast, a blue shift would have been expected, if Arg52 had played a role in charge stabilization. This suggests that electrostatic complementarity provided by the guanidinium group makes only a negligible contribution to the red shift of the chromophore between its free and protein-bound forms. In contrast, the Glu46Gln mutation, which alters the hydrogen-bonding network around the chromophore, has a stronger effect on PYP's color. This mutation increases the red shift of the chromophore by 16 nm, resulting in an absorption maximum at 462 nm. This change can be explained in terms of increased negative charge density on the chromophore. Previous pH titration experiments of chromophore bound to unfolded PYP showed that the generation of a negative charge on the chromophore leads to a red shift in its absorption spectrum (Baca et al., 1994). In the Glu46Gln mutant, the hydrogen bond between the chromophore's phenolic oxygen and the side chain of residue 46, which was of the O···H···O type, is replaced by a hydrogen bond of the O···H···N type. The glutamate side chain's oxygen is able to deprotonate readily, whereas deprotonation of a glutamine side chain's nitrogen is all but impossible. Therefore, the hydrogen atom shared in the chromophore−side chain hydrogen bond will be localized farther away from the chromophore in the mutant than it is in the wild-type protein. Consequently, the substitution of Glu46 by Gln would lead to a net increase in negative charge on the chromophore, resulting in the observed red shift. Stretching this hydrogen bond should result accordingly in an even higher concentration of charge on the chromophore. We propose, therefore, that the red shift in PYP's absorption spectrum during the formation of intermediate I1 (Meyer et al., 1987) is due to a distortion of the hydrogen-bonding network that stabilizes the charge of the chromophore in the ground state. On the other hand, a complete disruption of the ground state hydrogen-bonding network causes the chromophore to become protonated and shifts its absorption spectrum into the UV region, as apparently happens during the formation of the I2 intermediate (Genick et al., 1997).

Mutational Effects on Light Cycle Kinetics. On the basis of the ground state and intermediate I2 crystal structures, Genick et al. (1997) proposed a structural model for PYP's light cycle. In this model, the absorption of a photon triggers very rapid isomerization of the chromophore to form intermediate I1. The subsequent I1 → I2 transition involves the displacement of Arg52 from its original position and the exposure of the chromophore to solvent. This leads to proton uptake by the chromophore, which results in the loss of color. Subsequent reisomerization of the chromophore triggers the return of the colorless intermediate I2 to the ground state (P). From this model, the acceleration of the I1 → I2 transition observed for the Arg52Ala mutant can be readily understood. Truncation of the Arg52 side chain opens the way for the chromophore to assume its I2 position without having to displace the arginine side chain. The changes in the reaction rate and its pH dependence in the Glu46Gln mutant cannot be understood as easily, and further experiments will be needed to gain more detailed insight. Nevertheless, valuable information about PYP's photocycle was obtained from the spectroscopic experiments on Glu46Gln PYP. The kinetics of the I1 → I2 reaction and the spectral response curve of this mutant show that Glu46 still exerts an influence on the chromophore in I1, suggesting that the hydrogen bond between the side chain of Gln46 and the chromophore phenolic oxygen has not yet been completely disrupted. The very pronounced changes found in the rates of the I2 → P reaction for the Glu46Gln mutant were unanticipated. On the basis of our crystallographic experiments, we expected that the rate of the recovery reaction was largely dictated by spontaneous release of strain in the chromophore through reisomerization. The dramatic changes in the light cycle kinetics for both mutants indicate that this

is not the case. Thus, the present experiments demonstrate that the protein controls the speed of the back-reaction and that both Arg52 and Glu46 appear to be important in this control. The detailed mechanism by which PYP accelerates the back-reaction is however still unclear and merits further study.

Ionizable Groups in the Control of the Light Cycle. The bell-shaped curves for the pH dependence of the recovery reaction (I2 → P) rates in wild-type and Arg52Ala PYP (Figure 4) indicate that both acidic (apparent pK_a of 6.4) and basic (apparent pK_a of 9.4) groups control this reaction. PYP's active site lacks residues that normally exhibit these pK_a values in solution, but we know that PYP's protein environment can appreciably shift active site pK_a values, as demonstrated by deprotonation of the chromophore's phenolic oxygen and protonation of Glu46 in ground state PYP. Likewise, the observed pH dependence of PYP's kinetic properties may also depend on groups that exhibit abnormal pK_a values. The observed pH dependence for the Glu46Gln mutant (Figure 4) may result from complex interactions of ionizable groups. The removal of an ionizable carboxyl group introduced a dramatic pH dependence of the I2 → P recovery reaction dominated by a new pK_a of ∼8. Thus, in wild-type PYP, Glu46 appears to suppress or mask the ionization of the group responsible for the pK_a of 8 revealed in the Glu46Gln mutant. Active site residue Tyr42, which also forms a hydrogen bond to the chromophore's phenolic oxygen (Figure 1), may supply this ionizable group. This prediction can be tested in future mutagenesis experiments.

Conclusions. Our spectroscopic measurements of PYP's first site-directed mutants demonstrate the strong influence of specific interactions in the active site chemical environment on the light-sensing properties of this photoreceptor. This study shows that neither PYP's absorption spectrum nor its light cycle kinetics are controlled simply by physical properties inherent in the chromophore. Rather, the protein has evolved to modulate both of these properties to meet its hosts' biological needs. With the ability to choose the wavelength to which it responds and the rate by which it generates and turns off a structural signal, PYP presents itself as a highly evolved light receptor. We have identified some of the parameters that control the color and light cycle kinetics of PYP; additional studies will be necessary to determine the detailed mechanisms by which PYP controls its spectroscopic and kinetic properties.

REFERENCES

Baca, M., Borgstahl, G. E. O., Boissinot, M., Burke, P. M., Williams, D. R., Slater, K. A., & Getzoff, E. D. (1994) *Biochemistry 33*, 14369−14377.

Bogomolni, R. A., & Spudich, J. L. (1982) *Proc. Natl. Acad. Sci. U.S.A. 79*, 6250−6254.

Borgstahl, G. E. O., Williams, D. R., & Getzoff, E. D. (1995) *Biochemistry 34*, 6278−6287.

Genick, U. K., Borgstahl, G. E. O., Ng, K., Ren, Z., Pradervand, C., Burke, P. M., Srajer, V., Teng, T., Schildkamp, W., McRee, D. E., Moffat, K., & Getzoff, E. D. (1997) *Science* (in press).

Henderson, R., Baldwin, J. M., Ceska, T. A., Zemlin, F., Beckmann, E., & Downing, K. H. (1990) *J. Mol. Biol. 213*, 899−929.

Hoff, W. D., Düx, P., Hård, K., Devreese, B., Nugteren-Roodzant, I. M., Crielaard, W., Boelens, R., Kaptein, R., Van Beeumen, J., & Hellingwerf, K. J. (1994a) *Biochemistry 33*, 13959−13962.

Hoff, W. D., van Stokkum, I. H. M., van Ramesdonk, H. J., van Brederode, M. E., Brouwer, A. M., Fitch, J. C., Meyer, T. E., van Grondelle, R., & Hellingwerf, K. J. (1994b) *Biophys. J. 67*, 1691−1705.

Imamoto, Y., Ito, T., Kataoka, M., & Tokunaga, F. (1995) *FEBS Lett. 374*, 157−160.

Kim, M., Mathies, R. A., Hoff, W. D., & Hellingwerf, K. J. (1995) *Biochemistry 34*, 12669−12672.

Koh, M., van Driessche, G., Samyn, B., Hoff, W. D., Meyer, T. E., Cusanovich, M. A., & Van Beeumen, J. J. (1996) *Biochemistry 35*, 2526−2534.

Kort, R., Hoff, W. D., van West, M., Kroon, A. R., Hoffer, S. M., Vlieg, K. H., Crielaard, W., van Beeumen, J. J., & Hellingwerf, K. J. (1996) *EMBO J. 15*, 3209−3218.

Landt, O., Grunert, H. P., & Hahn, U. (1990) *Gene 96*, 125−128.

Meyer, T. E. (1985) *Biochim. Biophys. Acta 806*, 175−183.

Meyer, T. E., Yakali, E., Cusanovich, M. A., & Tollin, G. (1987) *Biochemistry 26*, 418−423.

Meyer, T. E., Tollin, G., Hazzard, J. H., & Cusanovich, M. A. (1989) *Biophys. J. 56*, 559−564.

Meyer, T. E., Cusanovich, M. A., & Tollin, G. (1993) *Arch. Biochem. Biophys. 306*, 515−517.

Oesterheldt, D., Tittor, J., & Bamber, E. (1992) *J. Bioenerg. Biomembr. 24*, 181−191.

Pace, C. N. (1975) *CRC Crit. Rev. Biochem. 3*, 1−43.

Schertler, G. F. X., Villa, C., & Henderson, R. (1993) *Nature 362*, 770−772.

Sprenger, W. W., Hoff, W. D., Armitage, J. P., & Hellingwerf, K. J. (1993) *J. Bacteriol. 175*, 3096−3104.

van Beeumen, J. J., Devreese, B. V., van Bun, S. M., Hoff, W. D., Hellingwerf, K. J., Meyer, T. E., McRee, D. E., & Cusanovich, M. A. (1993) *Protein Sci. 2*, 1114−1125.

BI9622884